



# Hydroelastic response of 19,000 TEU class ultra large container ship with novel mobile deckhouse for maximizing cargo capacity

Hong-II Im <sup>a,\*</sup>, Nikola Vladimir <sup>b</sup>, Šime Malenica <sup>c</sup>, Dae-Seung Cho <sup>d</sup>

<sup>a</sup> Hyundai Heavy Industries Co., Ltd., Ulsan, Republic of Korea

<sup>b</sup> University of Zagreb, Faculty of Mechanical Engineering and Naval Architecture, Zagreb, Croatia

<sup>c</sup> Bureau Veritas, Research Department, Paris, France

<sup>d</sup> Pusan National University, Department of Naval Architecture and Ocean Engineering, Busan, Republic of Korea

Received 12 August 2016; revised 24 October 2016; accepted 14 November 2016

Available online 8 December 2016

## Abstract

This paper is related to structural design evaluation of 19,000 TEU ultra large container ship, dealing with hydroelastic response, i.e. springing and whipping. It illustrates application of direct calculation tools and methodologies to both fatigue and ultimate strength assessment, simultaneously taking into account ship motions and her elastic deformations. Methodology for springing and whipping assessment within so called WhiSp notation is elaborated in details, and in order to evaluate innovative container ship design with increased loading capacity, a series of independent hydroelastic computations for container ship with mobile deckhouse and conventional one are performed with the same calculation setup. Fully coupled 3D FEM – 3D BEM model is applied, while the ultimate bending capacity of hull girder is determined by means of MARS software. Beside comparative analysis of representative quantities for considered ships, relative influence of hydroelasticity on ship response is addressed.

Copyright © 2016 Society of Naval Architects of Korea. Production and hosting by Elsevier B.V. This is an open access article under the CC BY-NC-ND license (<http://creativecommons.org/licenses/by-nc-nd/4.0/>).

**Keywords:** Structural design; Container ship; Hydroelastic approach; Springing; Whipping

## 1. Introduction

Structural design of 19,000 TEU Ultra Large Container Ship (ULCS) with open hold under novel mobile deckhouse for maximizing cargo capacity is evaluated in this paper, considering hydroelastic response, i.e. springing and whipping. Springing can be defined as the resonant hull girder vibration at the wave encounter frequency, while whipping is the transient hull girder vibration induced by slamming (other dynamic forces can also produce whipping, but slamming has dominant contribution). Springing is encountered mainly at moderate sea states where the combination of the wave frequencies and the ship speed might cause the closer matching

of the excitation and the structural natural frequencies, while whipping, is usually encountered in severe sea states where significant slamming events are likely to occur.

The practical procedure for ship structural design involves the verification of two main structural failure modes:

- Fatigue initiated cracks in the structure.
- Yielding and buckling failure due to extreme event.

These two failure modes are fundamentally different and the methodologies for their assessment differ despite some overlapping steps. The goal of the fatigue analysis is to assess the whole ship life by counting all the combinations of the stress ranges and number of cycles (S-N curves) for particular structural detail, while the final goal of the extreme event analysis is to predict, for each structural member, the single most likely worst event during whole ship life. It is to be noted

\* Corresponding author.

E-mail address: [okil@hhi.co.kr](mailto:okil@hhi.co.kr) (H.-I. Im).

Peer review under responsibility of Society of Naval Architects of Korea.

that, from hydroelasticity point of view, springing will mainly affect the structural fatigue life, while whipping can significantly affect both the fatigue and extreme structural responses.

As elaborated in a number of references as for instance (Malenica et al., 2013a,b; Malenica and Derbanne, 2014; Kim and Kim, 2014; Barhoumi and Storhaug, 2014; Senjanović et al., 2014a,b), springing and whipping are phenomena inherent to ULCS, and should be properly accounted for in their design procedure. However, there is no single methodology on this complex task and therefore some classification societies have recently developed relevant guidelines (ABS, 2010; LR, 2014; Bureau Veritas, 2015; DNV GL, 2015), dealing with representative sea state conditions, probability levels, ship speed approximations, structural and hydrodynamic modelling considerations, recommended numerical tools, etc. Such methodologies are regularly developed by combining the knowledge gained from numerical simulations, model tests and full-scale measurements (Malenica et al., 2011).

The evaluation of structural design of 19,000 TEU ULCS with open hold under mobile deckhouse (Im et al., 2014a,b, 2015; 2016) with hydroelastic effects included is a subject of this paper, and it is done at WhiSp1, 2 and 3 levels, respectively, according to the BV Rule Note 583 (Bureau Veritas, 2015). Beside outline of hydro-structure models, application of newly introduced WhiSp notation is elaborated in details and all calculations steps are illustrated within representative numerical examples. Full detailed description of innovative Container Ship (CS) concept with increased capacity and other ship characteristics is presented in (Im et al., 2016). A general hydro-structure tool combining 3D potential flow hydrodynamic model and 3D structural model is used (Malenica et al., 2013a; Sireta et al., 2013). The general numerical code Hydrostar (Bureau Veritas, 2006) is used as the hydrodynamic solver, and NASTRAN (MSC Software, 2010) as the structural solver. Fatigue lives and long term VBM values are calculated for the above mentioned ship with mobile deckhouse as well as for the conventional design and comparative analysis is performed.

## 2. Methodology description – springing and whipping assessment

### 2.1. Numerical models

The overall summary of the different aspects of the hydro-structure interaction models is shown in Table 1.

As it can be seen, a clear distinction is made in between the different types of the hydrodynamic loading (linear, weakly nonlinear and impulsive non-linear) and the two types of the structural responses (quasi-static and dynamic (hydroelastic)).

Table 1  
Different hydro-structural issues (H – hydrodynamics, S – structure).

H	Linear	Weakly nonlinear	Impulsive nonlinear
S			
Quasi static	X	X	X
Dynamic	X	X	X

It is very important to make this clear from the beginning because quite often in the literature some misunderstandings can be observed. This is mainly due to the fact that the hydrodynamic loading part is always dynamic however the structure could be or not be dynamically excited. In that respect we define here the quasi-static response as the one in which the ship structural vibrations are not taken into account while in the dynamic (hydroelastic) response they are included. Compared to quasi-static structural model, the hydroelastic model is significantly more complex because the hydrodynamic loading and the structural responses are depending on each other at each time instant so that fully coupled analysis is required. This is true regardless of the type of the hydrodynamic loading which is considered.

#### 2.1.1. Hydrodynamics

Before describing the hydroelastic model more in details let us first define different types of the hydrodynamic loading models. The linear hydrodynamic model is the one in which all the boundary conditions are linearized and the hydrodynamic Boundary Value Problem (BVP) is solved on a fixed domain. This model is usually solved in frequency domain which allows for very fast calculations. The weakly non-linear hydrodynamic model which is used here is the so called Froude Krylov model and it basically consists in correcting the hydrodynamic pressure close to the waterline. Indeed, according to the linear theory, the hydrodynamic model “stops” at the waterline ( $z = 0$ ) so that locally (close to the waterline), negative hydrodynamic pressures might occur. There exist different variants of the Froude Krylov model and the simplest one is rather intuitive and consists in adding the hydrostatic part of pressure below the wave crest (in linear sense) and by putting zero total pressure above the wave trough. The problem basically reduces to the evaluation of the (linear) wetted part of the ship at each time step, Fig. 1.

Finally, what we call the impulsive nonlinear hydrodynamic loading is the loading which is caused by different types of highly nonlinear local phenomena such as slamming, green water, underwater explosion and others. This loading is usually of transient character and shorter duration than the normal wave loading and that is why the hydroelastic analysis is usually required. In the present study the slamming loading only is considered within the context of the so called whipping phenomena. The slamming models represent the weakest part of the overall procedure because the slamming is extremely complex hydrodynamic problem and there is still no fully satisfactory 3D numerical solution available. For that reason, very often the so called strip approach is employed. Within this approach the different parts of the ship (most often forward and aft parts) are subdivided into different strips and on each of those strips the 2D slamming model (usually Generalized Wagner Model) is used. The input parameters for 2D slamming model (section position and velocity) are given by the global dynamic model at each time step. One example of the typical slamming sections is shown in Fig. 2. It is however important to note that, in spite of the weaknesses of the slamming model, its use in this particular case is more justified

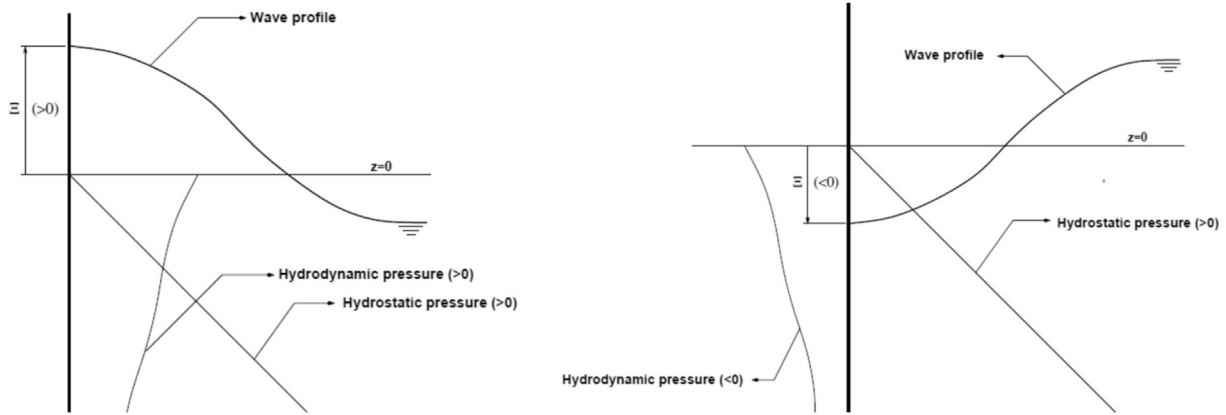


Fig. 1. Pressure correction near the waterline within the Froude Krylov approximation.

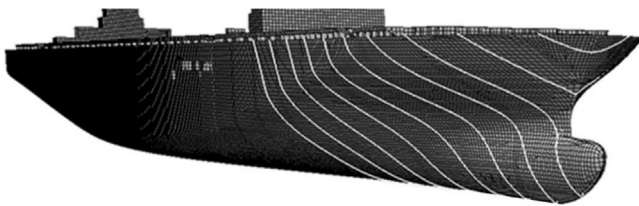


Fig. 2. Typical slamming sections for whipping model.

because we rely on comparative approach i.e. we are interested in the relative differences in between CS with open hold under mobile deckhouse and conventional CS designs only.

The used slamming module was recently significantly improved to reduce the computation time for slamming (De Lauzon et al., 2015). This reduction of CPU time for slamming was possible thanks to the use of the conformal mapping technique which, once performed, allows for the use of the Kelvin type of the Green's function for the solution of the associated boundary value problems. As shown in Fig. 3, the transformed configuration has the free surface position at the same level at both sides allowing the use of the Green function which satisfies the free surface condition explicitly (Kelvin Green function). In this way the meshing of the free surface is avoided and the number of unknowns is significantly reduced.

### 2.1.2. Hydroelasticity

The details of the implementation of the hydroelastic model in the general hydro-structure tool used in this analysis are

presented in (Malenica et al., 2013a) and here some basic aspects are outlined.

The hydroelastic model is based on the so called modal approach meaning that the global dynamic response of the structure can be represented as a sum of a limited number of the global ship structural modes (Bishop and Price, 1979). Within this approach the total ship displacement is represented as a series of the different modal displacements:

$$\mathbf{H}(\mathbf{x}, t) = \sum_{i=1}^N \xi_i(t) \mathbf{h}^i(\mathbf{x}) \quad (1)$$

where:

$\mathbf{H}(\mathbf{x}, t)$  total displacement of one point on the body.

$\mathbf{h}^i(\mathbf{x})$  modal displacements (mode shape).

$\xi_i(t)$  modal amplitude.

The modes are usually taken to be the structural natural modes and the rest of the procedure is very similar to rigid body analysis except that the number of degrees of freedom is increased from 6 to 6 plus a certain number of elastic modes. This modal approach implies the definition of supplementary radiation potentials with the following body boundary condition:

$$\frac{\partial \varphi_{Rj}}{\partial n} = \mathbf{h}^j \mathbf{n} \quad (2)$$

After solving the different boundary value problems for the potentials, the corresponding forces are calculated and the motion equation is written:

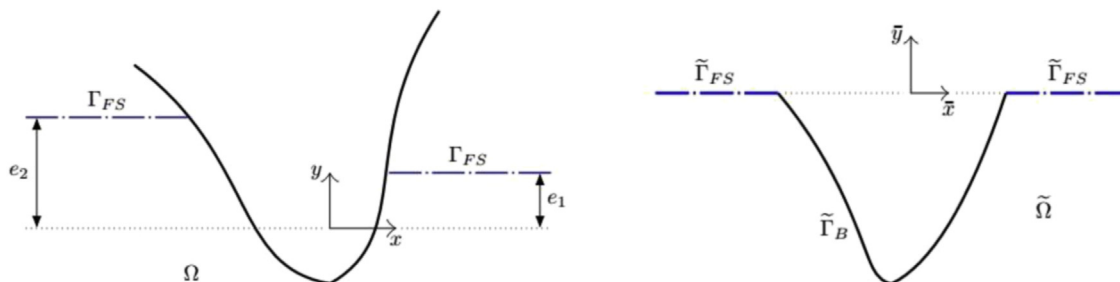


Fig. 3. Conformal mapping of the ship section (left – physical geometry, right – mapped geometry).

$$\{ -\omega^2([\mathbf{m}] + [\mathbf{A}]) - i\omega([\mathbf{B}] + [\mathbf{b}]) + ([\mathbf{k}] + [\mathbf{C}]) \} \{ \xi \} = \{ \mathbf{F}^{DI} \} \quad (3)$$

where  $[\mathbf{m}]$  is the modal structural mass,  $[\mathbf{b}]$  is the structural damping,  $[\mathbf{k}]$  is the structural stiffness,  $[\mathbf{A}]$  is the hydrodynamic added mass,  $[\mathbf{B}]$  is the hydrodynamic damping,  $[\mathbf{C}]$  is the hydrostatic restoring,  $\{ \xi \}$  are the modal amplitudes and  $\{ \mathbf{F}^{DI} \}$  is the modal hydrodynamic excitation.

Contrary to the quasi static case where the hydrodynamic pressure need to be transferred from the hydrodynamic mesh to the structural FE mesh, in the present case the radiation boundary condition (2) implies the transfer of the structural modal displacements from the structural mesh to the hydrodynamic mesh. The non-trivial interpolation procedure is necessary in order to perform this transfer and the typical result of this interpolation is shown in Fig. 4.

In principle, the solution of Eq. (3) gives the modal amplitudes so that the hydroelastic problem is formally solved. The great care should be given to the proper separation of the dynamic and the quasi-static parts of the structural responses. Due to the fact that only the limited number of structural modes is used, the final structural response cannot be obtained by simply summing the different modal contributions because, in most of the cases, the convergence will not be properly achieved. This means that all the modes which were not taken into account in the hydroelastic model should be accounted for in quasi-static manner. Within the numerical model which was implemented in the applied numerical tool, the decomposition of the quasi-static and dynamic parts of the response is done by first schematically rewriting the motion Eq. (3) in the following form:

$$\left( \begin{bmatrix} [\mathbf{RR}] & [\mathbf{RE}] \\ [\mathbf{ER}] & [\mathbf{EE}] \end{bmatrix} + \begin{bmatrix} [0] & [0] \\ [0] & [\mathbf{k}] \end{bmatrix} \right) \begin{Bmatrix} \xi^R \\ \xi^E \end{Bmatrix} = \begin{Bmatrix} \mathbf{F}^R \\ \mathbf{F}^E \end{Bmatrix} \quad (4)$$

where  $\mathbf{R}$  stands for the rigid body parts,  $\mathbf{E}$  for the elastic ones and  $\mathbf{k}$  is the modal structural stiffness. At the same time the total response amplitudes are separated into the quasi static (subscript 0) and dynamic (subscript  $d$ ) parts:

$$\xi^R = \xi_0^R + \xi_d^R, \quad \xi^E = \xi_0^E + \xi_d^E \quad (5)$$

The quasi static part of the responses is defined by the following equations:

$$\begin{aligned} [\mathbf{RR}] \{ \xi_0^R \} &= \{ \mathbf{F}^R \} \\ [\mathbf{k}] \{ \xi_0^E \} &= \{ \mathbf{F}^E \} - [\mathbf{ER}] \{ \xi_0^R \} \end{aligned} \quad (6)$$

After inserting (5) and (6) into (4), the following linear system of equations for dynamic parts is obtained:

$$\left( \begin{bmatrix} [\mathbf{RR}] & [\mathbf{RE}] \\ [\mathbf{ER}] & [\mathbf{EE}] \end{bmatrix} + \begin{bmatrix} [0] & [0] \\ [0] & [\mathbf{k}] \end{bmatrix} \right) \begin{Bmatrix} \xi_d^R \\ \xi_d^E \end{Bmatrix} = - \begin{Bmatrix} [\mathbf{RE}] \xi_0^R \\ [\mathbf{EE}] \xi_0^E \end{Bmatrix} \quad (7)$$

The above procedure is the key point for the modal approach and it allows for fully consistent evaluation of the total structural stresses. Indeed, the quasi static part of the stresses is calculated using the direct approach (Im et al., 2016), i.e. not modal approach, so that all the structural modes are included in the quasi static part of the stresses. This means that the higher order modes, which will not be excited by slamming, will be taken into account consistently. At the end of the procedure, the dynamic contribution, given by Eq. (7), is simply added to the quasi static part and the total stresses are obtained. Anyway, the proposed approach completely removes the convergence problems due to the incomplete series of modes which is used and, at the same time, allows for very clear separation of the classical quasi-static and hydroelastic contributions. This makes the analysis of the relative influence of hydroelasticity on the overall structural response, straightforward.

Once the linear hydroelastic model is solved in frequency domain, and similar to rigid body dynamics (Im et al., 2016), the time domain model is constructed following the well-known method proposed by Cummins (1962), and the different nonlinearities are added to the excitation at each time step. This allows for the inclusion of the slamming loads which are absolutely necessary for whipping simulations. The final dynamic equation is written in following form:

$$\begin{aligned} ([\mathbf{m}] + [\mathbf{A}^\infty]) \{ \ddot{\xi}(t) \} + ([\mathbf{k}] + [\mathbf{C}]) \{ \xi(t) \} + [\mathbf{b}] \{ \dot{\xi}(t) \} \\ + \int_0^t [\mathbf{K}(t-\tau)] \{ \dot{\xi}(\tau) \} d\tau = \{ \mathbf{F}(t) \} + \{ \mathbf{Q}(t) \}, \end{aligned} \quad (8)$$

where,

- $[\mathbf{m}]$  – modal mass matrix.
- $[\mathbf{A}^\infty]$  – infinite frequency modal added mass matrix.
- $[\mathbf{k}]$  – structural stiffness matrix.
- $[\mathbf{C}]$  – hydrostatic restoring matrix.

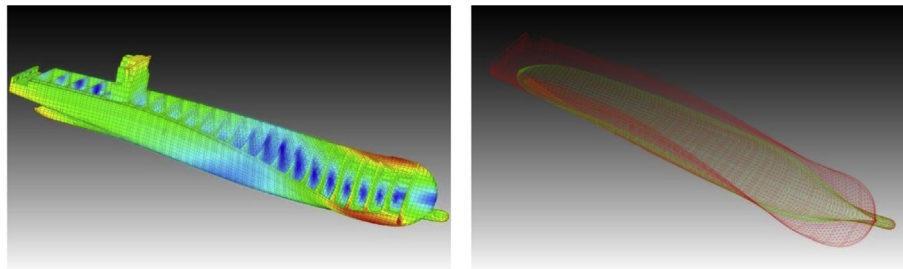


Fig. 4. First natural structural mode and transfer of the modal displacements from structural to hydrodynamic mesh.

- [**b**] – structural damping matrix.
- [**K**( $t - \tau$ )] – impulse response (memory) functions matrix.
- {**F**( $t$ )} – linear excitation force vector.
- {**Q**( $t$ )} – nonlinear excitation force vector.
- { **$\xi$** ( $t$ )} – body motions/deformations vector.

2.2. *WhiSp notation*

The WhiSp notation aims to take into account the influence of hydroelasticity on the ship structural response both from the fatigue and extreme response points of view. The details of the WhiSp notation are described in the Rule Note BV NR583 (Bureau Veritas, 2015). Among other technical issues, this note includes:

- Recommendations for springing and whipping assessment
- Methodology for the long term analysis of the different physical quantities
- Description of the different levels of the WhiSp notation

The field of application of the WhiSp notation is summarized in Table 2, where *Service feature* basically means mandatory and *Class notation* means optional.

The application of higher level of the WhiSp notation generally implies the application of the lower levels of the notation. This means that in the case when WhiSp2 notation is requested the WhiSp1 notation is mandatory and in the case when WhiSp3 notation is requested both WhiSp2 and WhiSp1 notations are mandatory.

In the following sections the meaning of each level of the WhiSp notation is briefly described.

2.2.1. *WhiSp1*

WhiSp1 notation is related to springing induced fatigue. The overall procedure is shown in Fig. 5.

As it can be seen, the definition of WhiSp1 is very simple and the same spectral fatigue methodology as the one used for quasi-static spectral fatigue is used. The only difference is that the linear hydroelastic response (springing) is included. In order to evaluate the local stress concentration at particular structural detail, the so called top-down analysis should be also used here (Sireta et al., 2012).

2.2.2. *WhiSp2*

WhiSp2 notation is related to the verification of the ultimate strength only, and it basically considers the evaluation of the influence of whipping on the extreme Vertical Bending Moment (VBM). It is very important to note that, within this

Table 2  
WhiSp notation.

	Container Ships		All other ships
	300 m < L < 350 m	L > 350 m	
WhiSp1	Service feature	Service feature	Class notation
WhiSp2	Class notation		
WhiSp3	Class notation	Class notation	Class notation

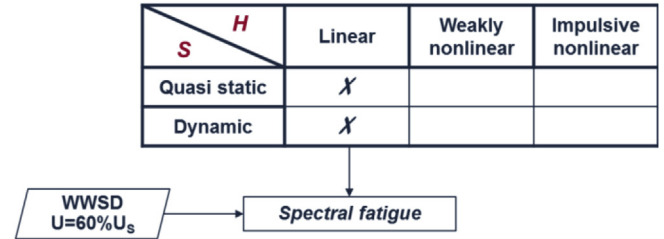


Fig. 5. Calculation procedure for WhiSp1 notation, (WWSD – World Wide Scatter Diagram, U – Ship speed, Us – Ship service speed).

notation, the ultimate strength only is concerned and the verification procedure for yielding and buckling strength remains the same as for the quasi static approach (see Im et al., 2016).

The overall calculation procedure for application of the WhiSp2 notation is shown in Fig. 6.

The procedure starts by the evaluation of the linear long term values of the Vertical Bending Moment (VBM) using the quasi-static approach. Once the long term value of the quasi static VBM has been evaluated, the corresponding Design Sea State (DSS) is defined. This DSS corresponds to the sea state with the most important contribution to the linear long term value of the VBM. For this DSS the nonlinear whipping simulations should be performed and the ratio with respect to the corresponding long term linear quasi static bending moment is defined. This ratio represents what is described as whipping correction in Fig. 6, and the same factor is then applied at the level of the ultimate strength structural response for all the ship sections.

Let us also mention that, in order to increase the convergence and reduce the calculation time, the concept of the so-called Increased Design Sea State (IDSS) is used for whipping calculations (we refer to NR583 (Bureau Veritas, 2015) for the detailed definition of the IDSS). Namely, simulation time is determined as a return period of the 25-years extreme

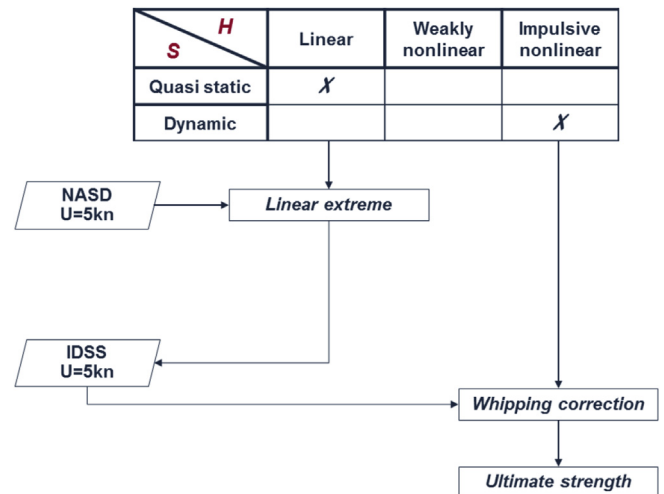


Fig. 6. Calculation procedure for WhiSp2 notation, (NASD – North Atlantic Scatter Diagram, IDSS – Increased Design Sea State).

VBM on DSS to get the reliable time domain results, which may lead to very long simulation. Therefore, the wave height is artificially increased, to reduce the return period of extreme VBM, while the wave period is kept at original value. In principle the above procedure fully covers the WhiSp2/3 notation and no additional calculations are necessary. However, in order to properly assess the relative influence of hydroelasticity on the values of the maximum vertical bending moment, usually one additional numerical simulation is performed. This additional simulation consists in performing the weakly nonlinear quasi-static simulation for the same IDSS as the one which was used for whipping simulations, as indicated in Fig. 7. In this way we are able to identify the pure rigid body nonlinear contribution (RB wave correction) to the total increase of the vertical bending moment and subsequently assess the relative influence of hydroelasticity.

2.2.3. WhiSp3

The WhiSp3 notation is dedicated to the evaluation of the influence of whipping on fatigue. The overall calculation procedure is shown in Fig. 8.

In the first step the classical spectral fatigue analysis with springing included (WhiSp1 notation) is performed. At the same time the Design Sea States (DSSS) are identified. These DSSS correspond to the sea states with the most important contribution to the fatigue. The whipping simulations are then performed on those sea states and the whipping correction coefficients for fatigue life are identified. The correction coefficients for other sea states are interpolated/extrapolated and the fatigue life is calculated by simple summation of the different contributions.

In the context of the application of WhiSp3 notation, it is important to discuss the way in which the time histories of the local structural stresses are calculated. Indeed, in order to allow for consistent comparisons of the damage induced by the quasi static and dynamic stresses we need to calculate the time histories of the local stresses, on which the rainflow counting method will be applied in order to evaluate the corresponding

<b>S \ H</b>	Linear	Weakly nonlinear	Impulsive nonlinear
Quasi static	X		
Dynamic	X		X

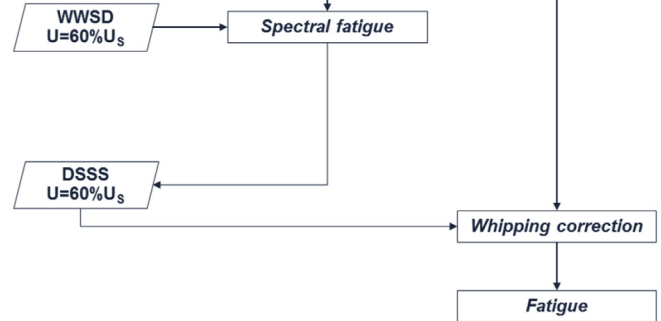


Fig. 8. Calculation procedure for WhiSp3 notation, (WWSD – World Wide Scatter Diagram, DSSS – Design Sea States).

fatigue lives. Due to the fact that the modal approach was used for the evaluation of the hydroelastic whipping response and since the retained number of modes is practically limited (10–15), the total local structural stresses cannot be fully accurately calculated by simple summation of the different modal contributions because the contribution of the higher modes will be missing. On the other hand, at least for the time being, we cannot afford for the direct evaluation of the stresses by solving the 3DFEM structural problem at each time step, because the required CPU time becomes prohibitive. For all these reasons, the stress time histories can be evaluated only approximately and there exist different ways to do that. The simplest method consists in retaining the modal contributions only, but more sophisticated methods based on the concept of the conversion matrices were also developed (Bigot et al., 2015). Since we are interested here in the ratio of the two types of the stresses (linear quasi static and whipping induced) only, we decided to apply the modal decomposition method for which we believe that it will give the quite fair first insight into the relative influence of whipping on fatigue. The more sophisticated methods for stress evaluation are left for further work.

3. Results and discussions

The calculation setup for hydroelastic analysis of two container ships having main particulars  $L_{pp} \times B \times T = 383.0 \times 58.6 \times 16.0$  m is exactly the same as the one applied in quasi-static analysis (see Im et al., 2016) following (Bureau Veritas, 2015, 2016). So, hydroelastic analyses of considered ships are performed for two ship speeds, i.e. 5.0 kn and 13.8 kn for ultimate strength (WhiSp2) and fatigue (WhiSp1 and 3) evaluation, respectively with uniformly distributed headings (from 0° to 350° with step of 10.0°) and wave frequencies (from 0.0 to 2.0 rad/s with frequency step of 0.01 rad/s), respectively. The position of the considered structural details is indicated in Fig. 9:

<b>S \ H</b>	Linear	Weakly nonlinear	Impulsive nonlinear
Quasi static	X	X	
Dynamic			X

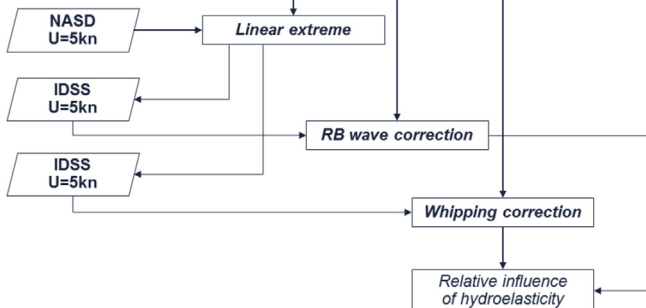


Fig. 7. Evaluation of the relative influence of hydroelasticity on the increase of the vertical bending moment.

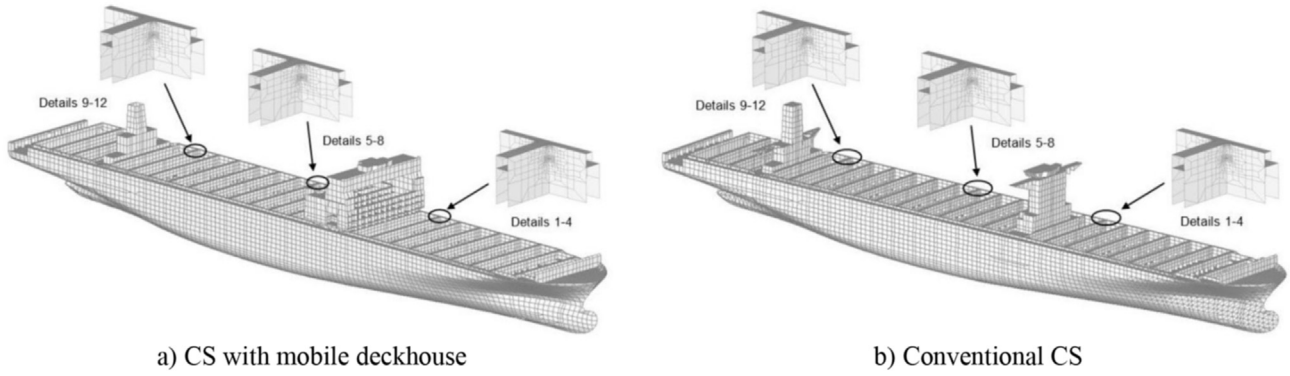


Fig. 9. 3D FE models of the analyzed container ships with local fine mesh models.

The first step in hydroelastic analysis is dry natural vibration analysis, with results summarized in Fig. 10, together with indicated values of wet natural frequencies for both ships.

### 3.1. Fatigue

Typical stress RAO obtained by hydroelastic computation and applying top-down approach is shown in Fig. 11 for elements 11 of both ships, where the elastic resonant peaks corresponding to 1T+HB natural mode are clearly visible. The results are obtained for structural damping equal to 2.0% and 7.0% of the critical damping for bending and torsional elastic modes, respectively.

After stress RAOs are computed, fatigue lives are calculated according to the same procedure as for quasi-static approach (see Im et al., 2016). Without going into details, Table 3 summarizes the ratios of fatigue lives of analyzed CSs, as well as the ratios of fatigue lives obtained by quasi-static and hydroelastic approach.

Similar to the quasi-static approach, conventional CS shows somewhat better performance from the viewpoint of fatigue with springing included (WhiSp1). Also, the effect of springing on the fatigue life differs from one detail to another,

depending on its position along the ship, its geometry, properties, etc., but generally one can see that in most cases springing has higher influence on structural details of CS with mobile deckhouse especially those located close to the deckhouse moving mechanism.

The natural frequencies are one of the reasons for higher fatigue damage for the CS with movable deckhouse but probably not the most important one. The main reason is the stress concentration close to the critical structural elements which is much higher in the case of CS with movable deckhouse. This can be seen from Fig. 11 where the RAO's of the stress in the elements 11 for both ships are presented.

In order to illustrate the application of WhiSp3 notation, i.e. to assess the influence of whipping on fatigue life, the calculation procedure described in Fig. 8 is applied to details 1, 8 and 11, respectively. In the first step of the WhiSp3 procedure, the most contributing operating conditions (i.e. the combinations of the sea state ( $H_s, T_p$ ) and the heading), are determined using the spectral fatigue analysis. In that respect, it is important to mention that each detail has its own most contributing operating conditions which means that the number of whipping simulations can become very large. Anyway, for all the considered DSSS, the time domain whipping

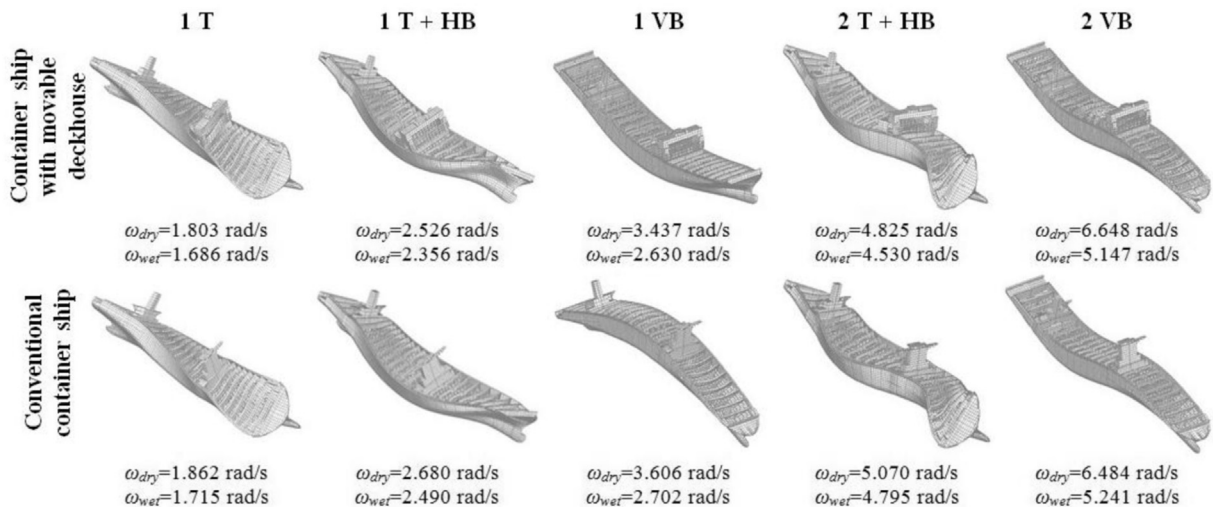


Fig. 10. Mode shapes and natural frequencies of analyzed container ships.

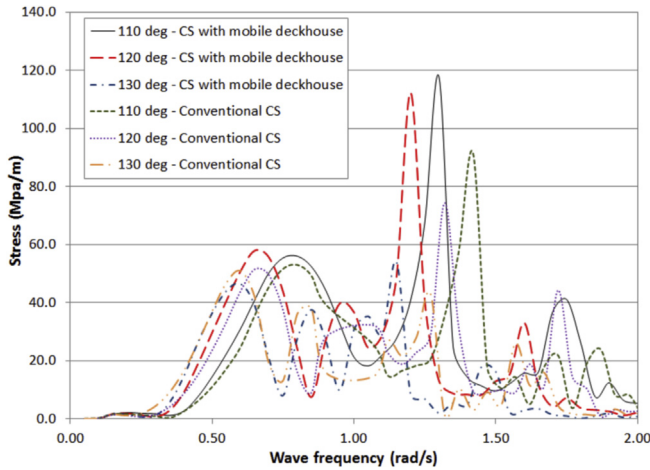


Fig. 11. Stress RAO sample with springing effect included for elements 11 of both analyzed ships.

simulations are performed and the short term stress time histories are produced. In parallel the time signals for the quasi static simulations are generated by the re-composition of the linear frequency domain results. The typical time signals are shown in Fig. 12 where we can clearly observe the influence of hydroelasticity. In the next step, the rainflow counting method is applied to all the signals in order to calculate the corresponding fatigue damage, and to deduce the different damage ratios (Table 4).

Similarly as for the influence of linear springing on fatigue, one can see from Table 4, that whipping influence on fatigue damage will differ from one detail to another. However, for the above details, contribution of whipping seems to be slightly more important in case of CS with mobile deckhouse.

### 3.2. Extreme

As already mentioned, within the WhiSp2 notation only the ultimate strength is of concern and yielding and buckling verifications remains the same as for the case without WhiSp

Table 3  
Comparison of fatigue damage of analyzed container ships.

Detail	Damage ratio (conventional CS/CS with mobile deckhouse)		Damage ratio (WhiSp1/quasi-static linear)	
	Quasi-static linear	WhiSp1	CS with mobile deckhouse	Conventional CS
1	1.46	1.14	1.51	1.18
2	0.60	0.67	5.18	5.77
3	1.25	0.58	3.97	1.85
4	0.76	0.29	2.95	1.15
5	1.00	0.90	1.27	1.14
6	0.87	0.83	1.24	1.19
7	0.86	0.82	2.30	2.20
8	0.63	0.51	2.53	2.04
9	0.84	0.89	1.95	2.07
10	0.58	0.72	2.16	2.68
11	0.74	0.76	1.87	1.94
12	0.96	0.90	2.11	1.97

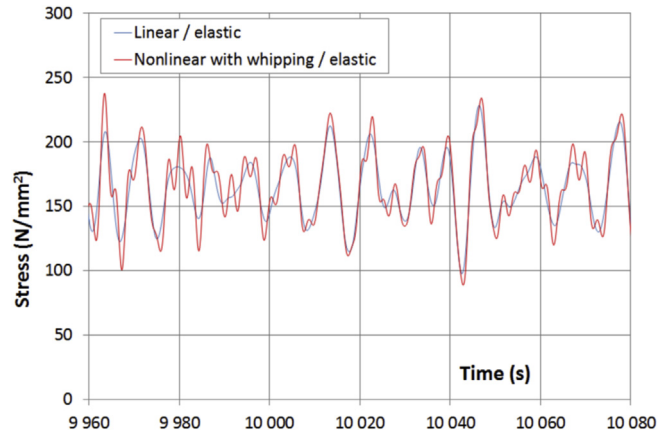


Fig. 12. Sample of stress time history in a structural detail.

Table 4  
Relative influence of hydroelasticity on fatigue damage of container ships.

Detail	Damage ratio (WhiSp3/quasi-static linear)	
	CS with mobile deckhouse	Conventional CS
1	3.83	3.21
8	2.77	2.46
11	2.01	2.34

notation. Extreme ship response is analyzed according to the procedure described in Fig. 6 (WhiSp2). Only one DLP, i.e. the vertical bending moment is taken into account with RAO shown in Fig. 13. IDSS concept is applied here and wave period and height for time domain simulation yield  $T_p = 16.19$  s and  $H_s = 16.92$  m, respectively. Typical VBM time histories, taking into account ship flexibility and slamming induced whipping are shown in Fig. 14 where the linear VBM is also presented for comparison. After postprocessing the different time signals the probability of occurrence of the different types of VBM is deduced and the final result is shown in Figs. 15 and 16.

From the long term values of the two VBM signals, the whipping correction coefficient is deduced and used to correct the linear long term value of the VBM in order to obtain the nonlinear long term value of extreme VBM which has to be used for the check of the ultimate strength. The different values of the VBM are summarized in Table 5.

According to the rules (Bureau Veritas, 2015) the ultimate check is performed by applying the following formula:

$$M \leq \frac{M_u}{\gamma_R}, \tag{9}$$

where  $M_u$  represents ultimate bending capacity of hull transverse section,  $M$  is computed extreme VBM and  $\gamma_R$  is partial safety factor taken equal to 1.1.

There are different ways to determine ultimate bending capacity of hull transverse section, and here for illustration rule based approach by using MARS (Bureau Veritas, 2000) software is applied, with corrosion margin included. Midship section of the both ships is the same, with thickness of plating

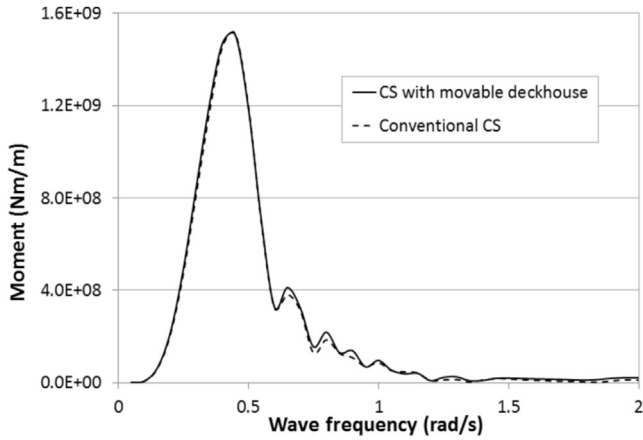


Fig. 13. RAOs of vertical bending moment at midship for head sea,  $U = 5.0$  kn.

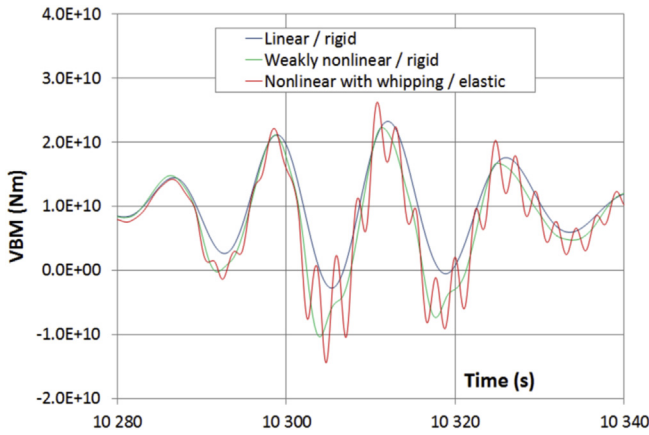


Fig. 14. Typical VBM time history at midship section of container ship.

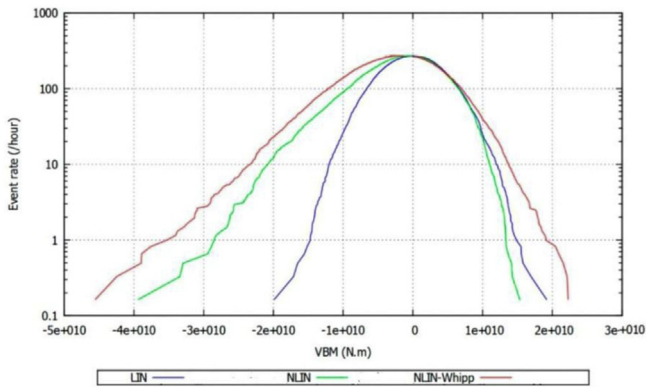


Fig. 15. VBM up-crossing extrema distribution for container ship with mobile deckhouse at midship.

indicated Fig. 17. Ultimate capacity of the ship determined by the MARS software yields  $3.37 \cdot 10^{10}$  Nm, and corresponds to the maximum of curve shown in Fig. 18. The right hand side of Eq. (9) yields  $3.06 \cdot 10^{10}$ , and if compared with corresponding long term VBM values from Table 5 for CS with mobile deckhouse ( $2.766 \cdot 10^{10}$  Nm) and conventional CS

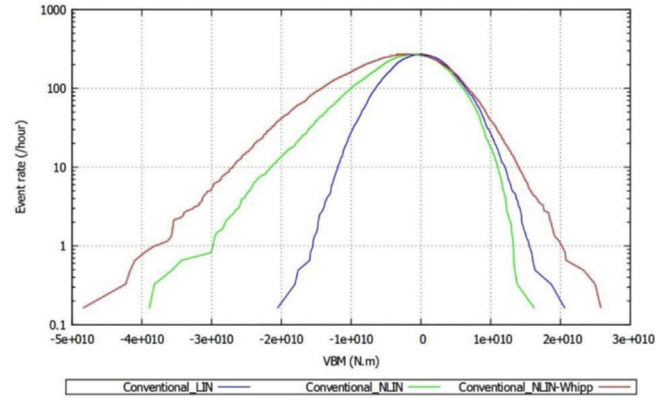


Fig. 16. VBM up-crossing extrema distribution for conventional container ship at midship.

( $2.865 \cdot 10^{10}$  Nm), it is obvious that global strength of both ships is at satisfactory level.

#### 4. Conclusion

The main goal of the present paper was to compare the structural integrity of two different concepts of the ultra large container ships, namely the conventional ship design and the newly developed innovative container ship with increased loading capacity. The main difference between two designs consist in the fact that, for new design, the deckhouse structure for accommodations is not fixed but is allowed to move longitudinally thanks to a special railing system. In this way the allowable cargo capacity is increased but the ship hull girder is made softer especially with respect to the torsional structural modes. The final consequence, from structural point of view, is that the structural natural frequencies are slightly lower, possibly leading to the increase of the dynamic stresses in the structure.

The comparisons were done within the direct calculation procedure covered according to (Bureau Veritas, 2015, 2016). In particular the WhiSp notations 1, 2 and 3 whose notations cover both the fatigue and the extreme structural strength were applied and allow for the consistent evaluation of the relative influence of hydroelasticity. As far as the extreme structural responses (yielding, buckling and ultimate strength) are concerned, both ships have similar behavior and both designs are safe. In the case of fatigue, the conventional design appears to have slightly better performance especially for the details located close to the mobile deckhouse mechanism. This is partly due to the lower torsional natural frequencies of the ship with mobile deckhouse but also to the differences in the local structural design which induce the larger local stress concentrations. However, this does not mean that the container ship with mobile deckhouse does not satisfy the fatigue criteria but some details should be investigated more carefully in order to decide whether the local structural modifications are necessary or not. In that respect, it is also important to note that, the present study considered the relative comparisons only and no quantitative values were given for fatigue life. This means that the conventional design was supposed to be safe from the

Table 5  
Long term values (25 years) of the VBM and the relative influence of whipping – WhiSp2 notation.

Item	CS with mobile deckhouse		Conventional CS	
	Sagging	Hogging	Sagging	Hogging
Still Water Bending Moment (SWBM)	1.023E + 10		9.928E + 09	
Quasi-static linear (without SWBM)	1.426E + 10		1.494E + 10	
Quasi-static nonlinear (without SWBM)	-2.542E + 10	1.328E + 10	-2.801E + 10	1.309E + 10
Whipping nonlinear (without SWBM)	-3.042E + 10	1.743E + 10	-3.434E + 10	1.872E + 10
Quasi-static total (with SWBM)	-1.519E + 10	2.351E + 10	-1.808E + 10	2.302E + 10
Whipping total (with SWBM)	-2.019E + 10	2.766E + 10	-2.441E + 10	2.865E + 10
Relative influence of Whipping	32.9%	17.7%	35.0%	24.5%

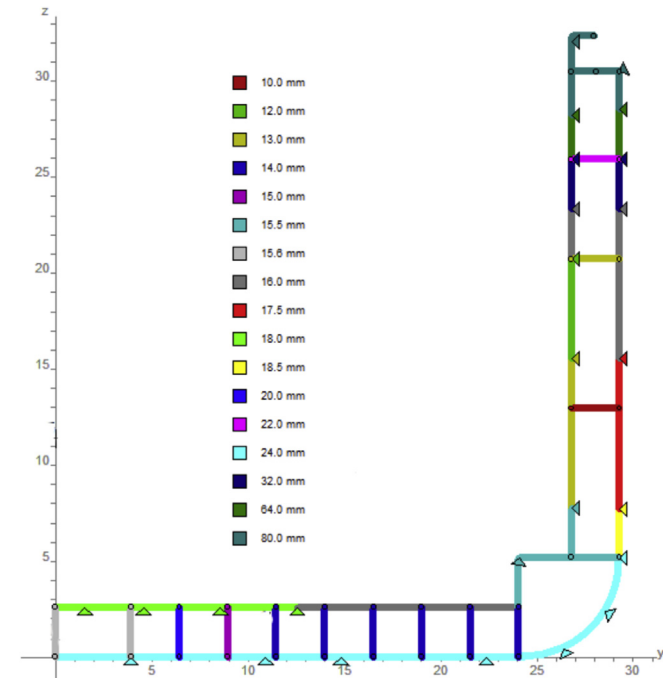


Fig. 17. Cross-section of considered ships (one half) with indicated plating thicknesses.

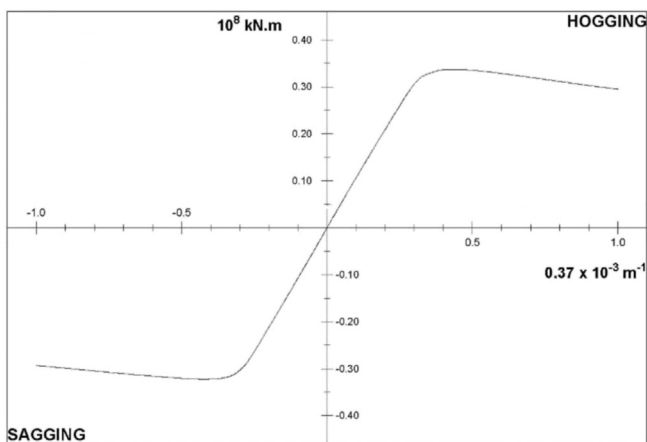


Fig. 18. Moment vs. curvature curve for container ship midship section.

fatigue point of view for all details. Further studies are necessary and will be carried out in order to evaluate more precisely the fatigue life of both ships.

**Acknowledgements**

This work was done within the Joint Research Project “A Study on Springing and Whipping of Hyundai SkyBench™ Container Carrier”. The authors would also like to acknowledge the support from a National Research Foundation of Korea (NRF) grant funded by the Korean Government (MSIP) through GCRC-SOP (Grant No. 2011-0030013). The obtained results and conclusions reflect personal opinions of the authors and do not represent official attitude of their institutions. Authors also acknowledge the support by Alexis Benhamou from Bureau Veritas Research Department for his valuable help.

**References**

ABS, 2010. Whipping Assessment for Container Carriers. American Bureau of Shipping, Houston, TX, USA.  
 Barhoumi, M., Storhaug, G., 2014. Assessment of whipping and springing on a large container vessel. *Int. J. Nav. Archit. Ocean Eng.* 6 (4), 442–458.  
 Bigot, F., Sireta, F.X., Baudin, E., Derbanne, Q., Tiphine, E., Malenica, S., 2015. A novel solution to compute stress time series in non linear hydro-structure simulations. In: *Proceedings of the 34th OMAE Conference* (Paper No. OMAE2015-42014), St. Johns, Canada.  
 Bishop, R.E.D., Price, G., 1979. *Hydroelasticity of Ships*. Cambridge University Press.  
 Bureau Veritas, 2000. MARS2000, User's Guide. Paris, France.  
 Bureau Veritas, 2006. Hydrostar, User's Manual. Paris, France.  
 Bureau Veritas, 2015. Whipping and Springing Assessment, Rule Note NR 583 DT R00 E. Paris, France.  
 Bureau Veritas, 2016. Structural Rules for Container Ships, Rule Note NR 625. Paris, France.  
 Cummins, W.E., 1962. The impulse response function and ship motions. *Schiffstechnik* 9 (47), 101–109.  
 De Lauzon, J., Grgic, M., Derbanne, Q., Malenica, S., 2015. Improved generalized Wagner model for slamming. In: *Proceedings of 7th International Conference on Hydroelasticity in Marine Technology*, Split, Croatia, pp. 561–574.  
 DNV GL, 2015. Class Guideline – DNVGL-CG-0153: Fatigue and Ultimate Strength Assessment of Container Ships Including Springing and Whipping.  
 Im, H.I., Cho, D.S., Kim, T.J., Choi, B.K., Ryu, H.R., Lee, B.R., 2014a. A new design of container carrier for maximizing cargo capacity. In: *Proceedings of International Conference Design and Operation of Container Ships*. RINA, London, UK, pp. 53–60.  
 Im, H.I., Cho, D.S., Hwang, G.H., Lee, D.H., Choi, B.K., Lee, B.R., 2014b. SkyBench™ container carriers for maximizing cargo capacity. In: *28th Asia Pacific Technical Exchange and Advisory Meeting on Mar Struct TEAM*, Istanbul, Turkey, pp. 508–513.  
 Im, H.I., Vladimir, N., Malenica, S., Ryu, H.R., Cho, D.S., 2015. Fatigue analysis of HHI SkyBench™ 19,000 TEU ultra large container ship with

- springing effect included. In: Proceedings of 7th International Conference on Hydroelasticity in Marine Technology, Split, Croatia, pp. 561–574.
- Im, H.I., Vladimir, N., Malenica, Š., Cho, D.S., 2016. Quasi-static Response of 19,000 TEU Class Ultra Large Container Carrier with Novel Mobile Deckhouse for Maximizing Cargo Capacity, Transactions of FAMENA, (Submitted).
- Kim, J.H., Kim, Y.H., 2014. Numerical analysis on springing and whipping using fully-coupled FSI models. *Ocean. Eng.* 91, 28–50.
- LR, 2014. ShipRight Design and Construction, Guidance Notes on the Assessment of Global Design Loads of Large Container Ships and Other Ships Prone to Whipping and Springing. Lloyd's Register, London, UK.
- Malenica, Š., Senjanović, I., Derbanne, Q., Vladimir, N., 2011. On the EU FP7 Project: tools for ultra large container ships – TULCS. *Brodogradnja* 62 (2), 177–187.
- Malenica, Š., Derbanne, Q., Sireta, F.X., Bigot, F., Tiphine, E., De Hauteclouque, G., Chen, X.B., 2013a. HOMER – Integrated hydro-structure interactions tool for naval and offshore applications. In: International Conference on Computers Applications in Shipbuilding, Busan, Korea.
- Malenica, Š., Senjanović, I., Vladimir, N., 2013b. Hydro structural issues in the design of ultra large container ships. *Brodogradnja* 64 (3), 323–347.
- Malenica, Š., Derbanne, Q., 2014. Hydro structural issues in the design of ultra large container ships. *Int. J. Nav. Archit. Ocean Eng.* 6 (4), 983–999.
- MSC Software, 2010. MD Nastran 2010 Dynamic Analysis User's Guide. Newport Beach, California, USA.
- Senjanović, I., Vladimir, N., Tomić, M., Hadžić, N., Malenica, Š., 2014a. Global hydroelastic analysis of ultra large container ships by improved beam structural model. *Int. J. Nav. Archit. Ocean Eng.* 6 (4), 1041–1063.
- Senjanović, I., Vladimir, N., Tomić, M., Hadžić, N., Malenica, Š., 2014b. Some aspects of structural modelling and restoring stiffness in hydroelastic analysis of large container ships. *Ships Offshore Struct.* 9 (2), 199–217.
- Sireta, F.X., Derbanne, Q., Bigot, F., Malenica, Š., Baudin, E., 2012. Hydroelastic response of a ship structural detail to seakeeping loads using a top-down scheme. In: Proceedings of the International Conference on Ocean, Offshore and Arctic Engineering – OMAE, ASME, Rio de Janeiro, Brazil.
- Sireta, F.X., De Lauzon, J., Surmont, F., 2013. HOMER User Guide. Bureau Veritas, Paris, France.